Macromolecular Research, Vol. 17, No. 9, pp 666-671 (2009)

# Water-Repellent Macroporous Carbon Nanotube/Elastomer Nanocomposites by Self-Organized Aqueous Droplets

**Bo Kyung Lim, Sun Hwa Lee, Ji Sun Park, and Sang Ouk Kim***

*Department of Materials Science and Engineering, KAIST Institute for the Nanocentury, Korea Advanced Institute of Science and Technology (KAIST), Daejeon 305-701, Korea*

*Received November 17, 2008; Revised February 2, 2009; Accepted February 6, 2009*

**Abstract:** Water repellent elastomeric surfaces were fabricated successfully on SBS/MWNT nanocomposites films using the breath figure method and subsequent thermal treatment. The uniformly dispersed CNTs were found to play significant roles in tuning the size and ordering of the macroporous morphology at the nanocomposite surface as well as enhancing the mechanical properties of nanocomposites. In particular, the CNTs dispersed in a nanocomposite solution retarded the coarsening process of aqueous droplets during the breath figure process and decreased the pore size in the finally fabricated film. The water contact angle measurement showed that the double-scale structure comprised of self-organized macropores and surface the roughness induced by a thermal treatment produced a highly water-repellent nanocomposite surface.

*Keywords*: carbon nanotubes, elastomer, nanocomposites, porous structure, water-repellency.

## Introduction

Thermoplastic elastomers (TPEs) compromise the good processibility of thermoplastic resin and rubber elasticity of crosslinked networks. The microphase-separated hard and soft segment domains provide moderate stiffness, optical transparency, as well as light weight. The properties of TPEs can be substantially reinforced with nanoscale fillers such as carbon nanotubes (CNTs),[1-5] clay platelets,[6] etc. In particular, TPE nanocomposites with uniformly dispersed CNTs may possess electrical conductivity, enhanced mechanical properties, and environmental stability.[2] The synergistic influence of CNTs upon TPEs has been widely exploited for potential applications in tissue engineering,[7] bio-scaffold,[8] high performance actuator,[1,9,10] and flexible electronic devices.[11,12]

The water-repellency of elastomeric materials is of great significance for electronic devices and corrosion protection. The design of antiwetting surfaces is commonly approached by fabricating micro-/nanostructures or employing materials with low surface energy.[13-15] The hierarchical structures with multi-scale orderings have been found to provide highly efficient hydrophobicity.[16] To fabricate artificial hydrophobic surfaces, various approaches have been proposed including templated fabrication,[17-21] fluorination,[22-24] and sol-gel method.[25] However, most of the previous approaches require complex chemical processes that frequently involve toxic chemical reagents.

*Corresponding Author. E-mail: sangouk.kim@kaist.ac.kr

We present a simple process for water-repellent TPE nanocomposites via self-organization of aqueous droplets and following thermal treatment. The homogeneous dispersion of multi-walled carbon nanotubes (MWCNTs) in a TPE matrix was achieved by the noncovalent functionalization of CNTs.[26,27] Amine-terminated polystyrene (PS-$NH_2$) were noncovalently grafted to the defect site of CNTs such that the resulting functionalized CNTs were homogeneously dispersed in a styrene-butadiene-styrene (SBS) TPE. The 'breath figure' method utilizing the spontaneous organization of aqueous droplets upon volatile polymer solution has been applied to the macroporous structure in the nanocomposite films.[28-30] The reinforcement of mechanical properties and water-repellency of macroporous nanocomposites was investigated as a functional of CNT content.

## Experimental

**Mateirlas.** MWNTs were purchased from Iljin Nanotec, Inc. Benzene was purchased from Merck. Monodisperse amine terminated polystyrene (PS-$NH_2$) having an Mw of 2,800 g/mol (PDI 1.15) were purchased from Polymer Source, Inc. Styrene-butadiene-styrene triblock copolymer (SBS) was provided by LG chemical Co. GPC (gel permeation chromatography) measurement of SBS provided an Mw of 118 Kg/mol and a PDI of 1.419, respectively. All materials except MWNTs were used without further purification. MWNTs were purified by sonication in a mixture of sulfuric acid and nitric acid (volume ratio of 3:1) for 10 h. The tem-

perature of the acid solution was maintained at about 60~70 °C. Upon sonication, metal catalysts were removed, and a limited number of carboxyl functional groups were formed at the edges and side walls of the MWNTs. Amorphous carbon and residual acid solutions were removed by subsequent heat treatment at 400 °C which continued for 40 min under atmospheric conditions.

**Preparation of Flat SBS/MWNTs Composite Films.** To prepare the nanocomposites, the mixture of SBS (Mw: 118 Kg/mol) and PS-$NH_2$ were used as a dispersant of the MWNTs. The weight ratio of dispersant to matrix SBS was 1:9. The purified MWNTs of various concentrations (0.2~3.2 wt% compared to matrix) were dispersed in the benzene solution of SBS/PS-$NH_2$ (4 wt%) by sonication. The prepared dispersion was spin-coated on a dichloromethylsilane treated silicon substrate to prepare a nanocomposite film.

**Porous Structure Fabrication and the Following Thermal Treatment.** A polymer solution including 3.6 wt% of SBS, 0.4 wt% PS-$NH_2$, and various amounts of MWNTs (0.2~3.2 wt%) was dropped on an organically modified silicon wafer surface under a stream of humid air (relative humidity of 80%, air flow rate of 3 L $min^{-1}$) at room temperature. The solution was left in the stream of humid air until it completely dried. After the formation of a porous structure, thermal treatment was performed at 50 °C for 60 min.

**Characterization.** Tensile tests were carried out on thin-film samples with dimensions of 40×10×0.3 $mm^3$ using a Instron 5583 mechanical tester with a 500 N load cell at a constant crosshead speed of 500 mm/min. Various surface morphologies of SBS/MWNT nanocomposites were investigated using a field emission scanning electron microscopy (FE-SEM, HITACHI 4800) at an accelerating voltage of 5 kV. The difference of wetting properties depending on surface treatments was measured using a contact angle analyzer in a static mode (Phoenix 150, SEO).

## Results and Discussion

Figure 1 schematically summarizes the procedures for SBS/MWNT nanocomposite films. To disperse MWNTs homogeneously, noncovalent functionalization of MWNTs was conducted. MWNTs were purified by a commonly applied process of acid treatment and subsequent thermal treatment. The purified MWNTs were dispersed in the benzene solution of SBS, including a small part of PS-$NH_2$ as a dispersant. The prepared solution was spin-coated on a silicon substrate to investigate the enhanced material properties of uniform nanocomposite films (Figure 1(a)). The ordered microporous polymer films have been prepared by the spontaneous organization of aqueous droplets (Figure 1(b)). The polymer composite solution was dropped on a silicon substrate under a stream of humid air. As the solvent evaporated, aqueous droplets condensed on the polymer solution surface and spontaneously organized into hexagonally packing. After evaporating the solvent and water completely, a highly ordered polymer thin film was obtained. The subsequent thermal treatment enhanced the roughness of the macroporous film surface such that they showed remarkably improved water-repellency.

To demonstrate the quantitative reinforcing effect of MWNTs

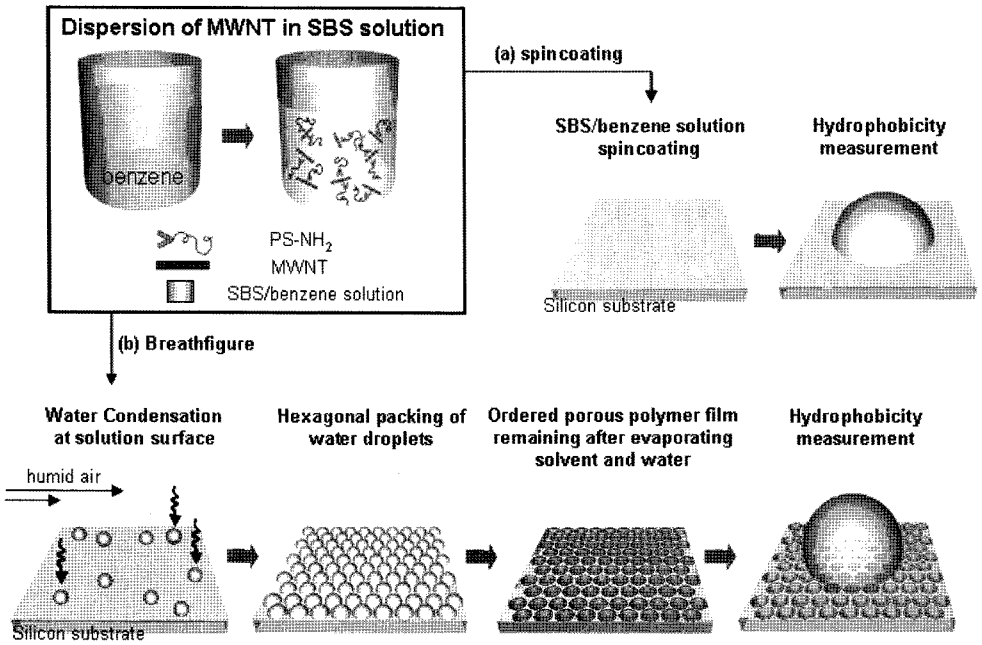


**Figure 1.** Experimental procedure for fabricating SBS/MWNT composite films (a) by spin coating or (b) by organization of aqueous droplets.

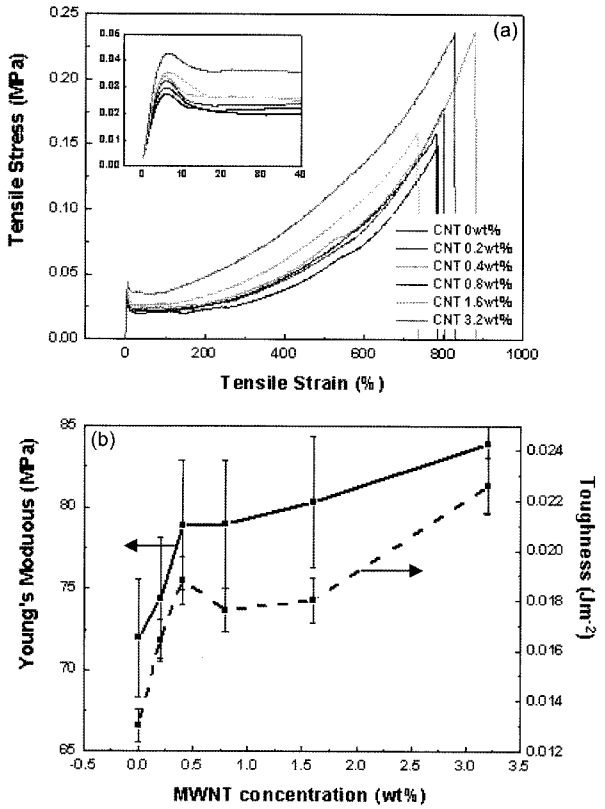


**Figure 2.** The mechanical properties of SBS with various concentration of MWNTs. (a) Representative engineering stress-strain curves of thin film nanocomposites including 0~3.2 wt% MWNT. (b) Young's modulus and the resistance to fracture provided the area underneath the stress-strain curve. Mechanical Percolating threshold concentration of MWNTs was 0.4 wt% according to the change of inclination.

upon the mechanical properties of the CNT/SBS nanocomposite films, tensile measurements were performed for the free-standing nanocomposite films. Figure 2(a) presents the strain-stress ($\sigma$-$\varepsilon$) curves of the various MWNT/SBS composite films. All curves exhibit typical rubber elastic behaviors. After yield behaviors, the slope of the curves monotonically increases up to the ultimate strain for break over 700%. As summarized in Figure 2(b), both the modulus and toughness of the nanocomposites increased with the amount of well-dispersed MWNTs. The mechanical percolation threshold appeared around the MWNT content of 0.4 wt%, above which the enhancement of mechanical properties was profoundly retarded.

Figure 3 shows the influence of the MWNT content upon the morphology of the macroporous nanocomposite films. In the preparing benzene solution, the concentration of SBS or amine-terminated PS was fixed at 3.6 or 0.4 wt%, respectively, which was determined as the optimized values for the well-ordered macroporous films. The insets are the SEM images of the composite films corresponding to each concentration. Without any MWNT, the mean pore diameter was about 5 μm and the lateral ordering of polydisperse pores included a high density of defects. The mean pore diameter decreased, and its distribution became more uniform, leading to an improved lateral ordering of pores with the MWNT content. The variation of pore size demonstrates a significant transition at 0.4 wt%, consistent with the percolation threshold for mechanical properties. The mean pore diameter rapidly decreased to 3 μm, the value at the 0.4 wt%, after which the decreasing rate became profoundly retarded. Due to the facile process and versatility, the 'breath figure' is a widely applied self-assembly method to prepare well-ordered macroporous polymer films over a large area.[26,27] In a 'breath figure' process, aqueous droplets condense upon a volatile solution surface and continuously coarsen each other. The degree of coarsening determines the final pore size. The mechanically percolated CNTs dispersed in a nanocomposite solution retarded the coarsening process and thereby decreased the pore size in the finally fabricated film.

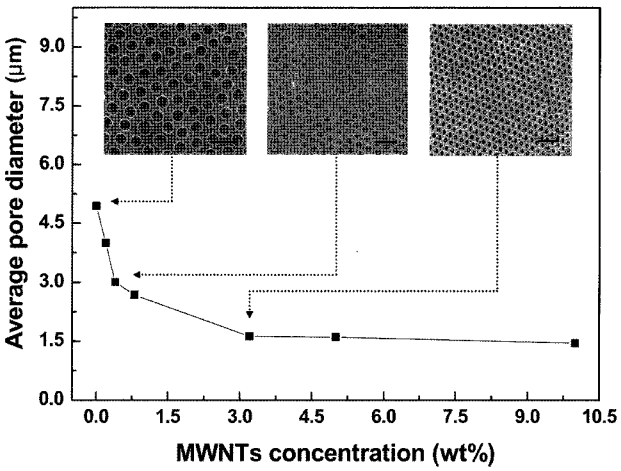


**Figure 3.** Average pore sizes in the porous SBS composite films according to the addition of various concentrations (0~10 wt%) of MWNTs. The insets are SEM images corresponding to each concentration. Scale bar is 10 μm. Pore size threshold concentration of MWNT was 0.4 wt% when pore diameter was 3 μm.

Figure 4 shows SEM images of macroporous films before and after thermal treatment. The thermal treatment was performed at 50 °C for 60 min. Figures 4(a) shows a tiled view of a porous morphology before the annealing process. We note that this regular porous morphology of elastomeric nanocomposites demonstrated almost permanent aging durability under ambient conditions, where the morphology was stable for more than six months. Since breath figure is an extremely rapid process accompanying the freezing of polymer molecules in a supercooled state, the breath figure morphology of ordinary brittle polymers such as polystyrene or poly(methyl methacylate) frequently shows a low structural stability with physical aging at an ambient temperature (Figure 5). By contrast, SBS TPE exhibited excellent stabil-

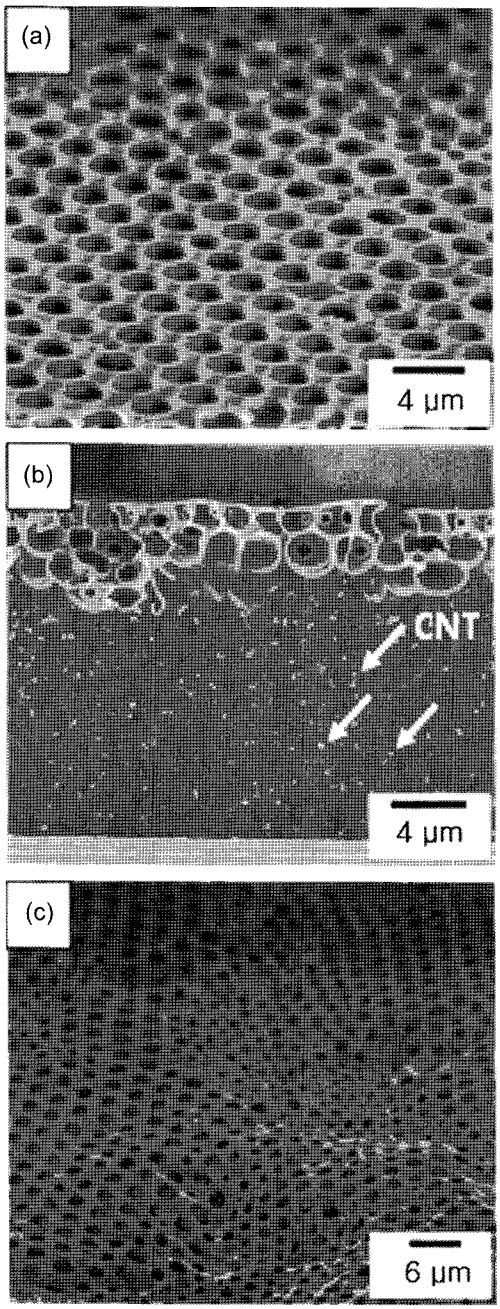


**Figure 4.** Ordered porous morphology of (a) SBS film in 60° tilting view, (b) is a cross section image of porous SBS/MWNT 3.2 wt% multilayer film. White spots indicated by white arrows show highly dispersed MWNTs in a composite film (c) SEM image of a porous film (b) after annealing for 60 min.

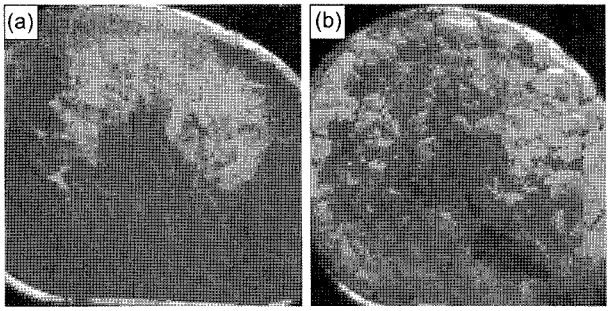


**Figure 5.** Structural stability of PS porous films at ambient temperature. The image of (a) breath figure film is after condensation of aqueous droplets. The collapsed morphology of (b) image was obtained after 20 days at ambient temperature.

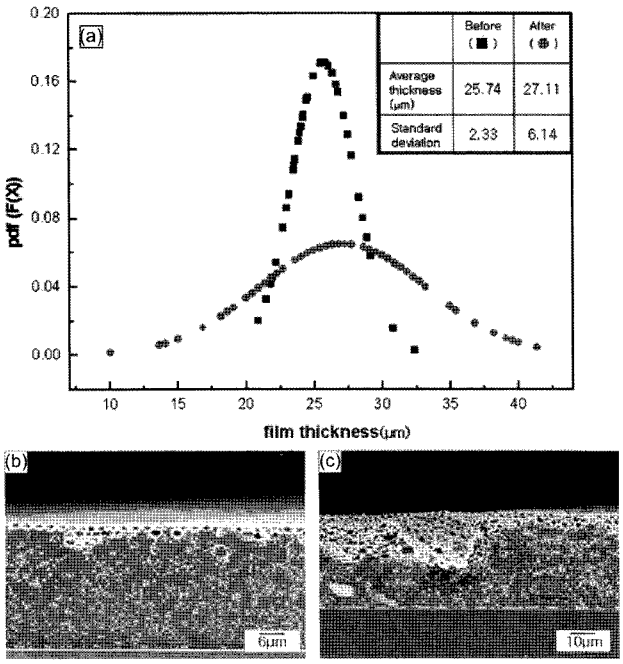


**Figure 6.** Quantitative analysis of the film roughness before and after annealing. (a) graph shows nominal distribution of SBS composite films including 3.2 wt% of MWNTs. Probability density function of the (b) film before annealing indicates flatter surface with narrow distribution of film thickness. Contrastively, broad curve expresses higher surface roughness of the annealed film (c) with much higher standard deviation value.

ity due to the easy deformability of the rubbery polybutadiene domains. The cross-sectional image of a porous elastomer film (Figure 4(b)) reveals the multi-layer structure of the porous morphology. Two or three layers of pores covered the top surface of the film. The image also presents the uniform dispersion of the noncovalently functionalized MWNT in the SBS matrix. Figure 4(c) presents the tilted view of a nanocomposite film after thermal treatment. The thermal treatment at 50 °C resulted in an extremely rough elastomer surface (Figure 6). Since the annealing temperature of 50 °C is above the glass transition temperature of rubbery PB domains and below the glass transition temperature of hard PS domains, the thermal deformation of microporous film is attributed to the relaxation of glassy PS domains. The thermal relaxation of the glassy domain resulted in a spin-coating process did not cause any significant morphological change under a prolonged thermal treat-

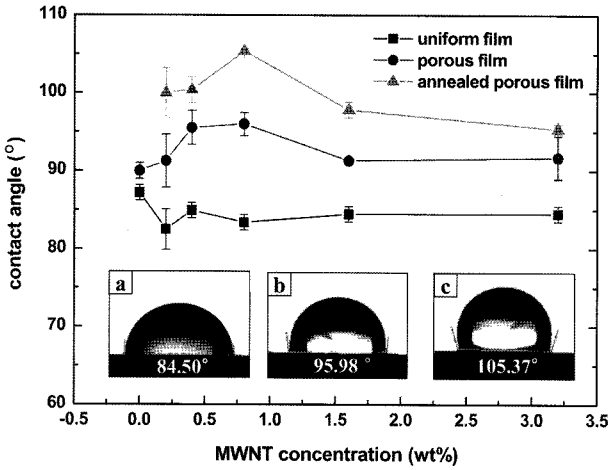


**Figure 7.** Contact angles with various concentrations of MWNTs. Inset images are water droplet shapes on the composite films of 0.8 wt% MWNTs concentration (a) flat surface, (b) porous surface, (c) porous surface after annealing for 60 min. The average diameter of the droplets is approximately 2.5 mm.

ment process.

The water-repellency of the elastomeric surface was characterized by contact angle measurement (Figure 7). As mentioned above, water-repellency is a crucial property for application to water-proof coatings or flexible electronics. The uniform nanocomposite films prepared by the spin-coating process showed a moderate contact angle of about 85°. The MWNT content did not significantly influenced the contact angle; however, introducing porous structure by the breath figure method increased the contact angle up to about 95°.

The porous structure has a role of air pockets under aqueous drops, which dramatically reduce solid-liquid contact area and thus enhanced the hydrophobicity. Remarkably, the thermally treated porous film showed the highest contact angle of about 105°. The surface roughness induced by the thermal treatment subsequently enhanced the water-repellency.

## Conclusions

In summary, water-repellent SBS/MWNT elastomeric nanocomposites have been successfully fabricated by the breath figure method and subsequent thermal treatment. This facile and versatile method can be applied to various thermoplastic polymers with an appropriate solution system. Most significantly, CNT content has been found to play important roles in tuning the size and ordering of macroporous morphology as well as enhancing mechanical properties. From the water contact angle measurement, it has been found that the double-scale structure comprising self-organized macropores and surface roughness induced by a thermal treatment endowed the highly water-repellent nanocomposite surface. Our versatile approach provides hydrophobic thermoplastic elastomer/CNT nanocomposites, potentially useful for diverse applications such as water-proof coatings, textile electronics, flexible electronics, etc.

**Acknowledgment.** This work was supported by the second stage of the Brain Korea 21 Project, the National Research Laboratory Program (R0A-2008-000-20057-0), the 21st Century Frontier Research Program (Center for Nanoscale Mechatronics and Manufacturing, 08K1401-01010), the Korea Science and Engineering Foundation (KOSEF) grant (R11-2008-058-03002-0), and the Fundamental R&D Program for Core Technology of Materials funded by the Korean government (MEST & MKE).

## References

(1) H. Koerner, G. Rice, N. A. Pearce, M. Alexander, and R. A. Vaia, *Nature*, **3**, 115 (2004).
(2) L. Bokobza, *Polymer*, **48**, 4907 (2007).
(3) X. B. Xu, Z. M. Li, L. Shi, X. C. Bian, and Z. D. Xiang, *Small*, **3**, 408 (2007).
(4) B. S. Kim, K. D. Suh, and B. Kim, *Macromol. Res.*, **16**, 76 (2008).
(5) I. Park, M. Park, J. Kim, H. Lee, and M. S. Lee, *Macromol. Res.*, **15**, 498 (2007).
(6) S. M. Liff, N. Kumer, and G. H. Mckinley, *Nature*, **6**, 76 (2007).
(7) R. H. Baughman, *Science*, **308**, 63 (2005).
(8) Y. Liu, K. J. Gilmore, J. Chen, V. Misoska, and G. G. Wallace, *Chem. Mater.*, **19**, 2721 (2007).
(9) R. Vaia, *Nature*, **4**, 429 (2005).
(10) S. V. Ahir and E. M. Terentjev, *Nature*, **4**, 491 (2005).
(11) H. J. Lee, Y. D. Lee, W. S. Cho, B. K. Ju, Y. H. Lee, J. H. Han, and J. K. Kim, *Appl. Phys. Lett.*, **88**, 093115 (2006).
(12) T. Sekitani, Y. Noguchi, K. Hata, T. Fukushima, T. Aida, and T. Someya, *Science*, **321**, 1468 (2008).
(13) R. Blossey, *Nature*, **2**, 301 (2003).
(14) X. Feng and L. Jiang, *Adv. Mater.*, **18**, 3063 (2006).
(15) H. Y. Lee, S. A. Yu, K. H. Jeong, and Y. J. Kim, *Macromol. Res.*, **15**, 547 (2007).
(16) Y. Lee, S. H. Park, K. B. Kim, and J. K. Lee, *Adv. Mater.*, **19**, 2330 (2007).
(17) L. Jiang, Y. Zhao, and J. Zhai, *Angew. Chem. Int. Ed.*, **43**, 4338 (2004).
(18) L. Feng, S. Li, Y. Li, H. Li, L. Zhang, J. Zhai, Y. Song, B. Liu, L. Jiang, and D. Zhu, *Adv. Mater.*, **14**, 1857 (2002).
(19) Y. Li, C. Li, S. O. Cho, G. Duan, and W. Cai, *Langmuir*, **23**, 9802 (2007).
(20) Y. Li, W. Z. Jia, Y. Y. Song, and X. H. Xia, *Chem. Mater.*, **19**, 5758 (2007).
(21) H. Li, Z. Wang, Y. Song, Y. Liu, Q. Li, L. Jiang, and D. Zhu, *Angew. Chem. Int. Ed.*, **40**, 1743 (2001).
(22) I. Woodward, W. C. E. Schofield, V. Roucoules, and J. P. S. Badyal, *Langmuir*, **19**, 3432 (2003).
(23) J. Genzer and K. Efimenko, *Science*, **290**, 2130 (2000).
(24) S. R. Coulson, I. Woodward, and J. P. S. Badyal, *J. Phys.*

*Chem. B*, **104**, 8836 (2000).
(25) K. Tadanaga, J. Morinaga, A. Matsuda, and T. Minami, *Chem. Mater.*, **12**, 590 (2000).
(26) S. H. Lee, J. S. Park, C. M. Koo, B. K. Lim, and S. O. Kim, *Macromol. Res.*, **16**, 261 (2008).
(27) S. H. Lee, J. S. Park, B. K. Lim, and S. O. Kim, *J. Appl. Polym. Sci.*, **110**, 2345 (2008).
(28) H. T. Ham, I. J. Chung, Y. S. Choi, S. H. Lee, and S. O. Kim, *J. Phys. Chem. B*, **110**, 13959 (2006).
(29) J. S. Park, S. H. Lee, T. H. Han, and S. O. Kim, *Adv. Funct. Mater.*, **17**, 2315 (2007).
(30) H. Yabu and M. Shimomura, *Chem. Mater.*, **17**, 5231 (2005).